HHS Public Access

Author manuscript

Neuroradiology. Author manuscript; available in PMC 2018 February 05.

Published in final edited form as:

Neuroradiology. 2018 January ; 60(1): 61–69. doi:10.1007/s00234-017-1949-1.

Functional brain networks involved in decision-making under certain and uncertain conditions

Danielle C. Farrar[1], **Asim Z. Mian**[2], **Andrew E. Budson**[3], **Mark B. Moss**[1], and **Ronald J. Killiany**[1]

[1]Department of Anatomy and Neurobiology, Boston University School of Medicine, 650 Albany St, Basement, Boston, MA 02118, USA

[2]Department of Radiology, Boston University School of Medicine, Boston, MA, USA

[3]VA Boston Healthcare System, Boston, MA, USA

Abstract

Purpose—The aim of this study was to describe imaging markers of decision-making under uncertain conditions in normal individuals, in order to provide baseline activity to compare to impaired decision-making in pathological states.

Methods—In this cross-sectional study, 19 healthy subjects ages 18–35 completed a novel decision-making card-matching task using a Phillips T3 Scanner and a 32-channel head coil. Functional data were collected in six functional runs. In one condition of the task, the participant was certain of the rule to apply to match the cards; in the other condition, the participant was uncertain. We performed cluster-based comparison of the two conditions using FSL fMRI Expert Analysis Tool and network-based analysis using MATLAB.

Results—The uncertain > certain comparison yielded three clusters—a midline cluster that extended through the midbrain, the thalamus, bilateral prefrontal cortex, the striatum, and bilateral parietal/occipital clusters. The certain > uncertain comparison yielded bilateral clusters in the insula, parietal and temporal lobe, as well as a medial frontal cluster. A larger, more connected functional network was found in the uncertain condition.

Conclusion—The involvement of the insula, parietal cortex, temporal cortex, ventromedial prefrontal cortex, and orbitofrontal cortex of the certain condition reinforces the notion that certainty is inherently rewarding. For the uncertain condition, the involvement of the prefrontal cortex, parietal cortex, striatum, thalamus, amygdala, and hippocampal involvement was expected, as these are areas involved in resolving uncertainty and rule updating. The involvement of occipital

Compliance with ethical standards

Conflict of interest AEB has been an investigator for clinical trials for the following companies: AstraZenica, Hoffmann-La Roche, Eli Lily, FORUM Pharmaceuticals, Avanir, Axovant, and Neuronetrix. MBM serves as a consultant for Pfizer, Inc. AZM is a shareholder of Boston Imaging Core Lab.

Ethical approval All procedures performed in studies involving human participants were in accordance with the ethical standards of the institutional and/or national research committee and with the 1964 Helsinki declaration and its later amendments or comparable ethical standards.

Informed consent Informed consent was obtained from all individual participants included in the study.

cortical involvement and midbrain involvement may be attributed to increased visual attention and increased motor control.

Keywords

Decision-making; fMRI; Executive function

Introduction

On a daily basis, individuals are faced with a multitude of decisions such as selecting the best route to reach a destination or choosing an investment strategy to optimize profit. In order to make these decisions, they ultimately must apply rules. Uncertainty regarding the optimal rule to apply to reach the desired outcome is often inherent in the decision-making process. Resolving this uncertainty is one of the most challenging components of the decision-making process. Being able to make decisions under conditions of rule uncertainty is vital to independent living and the impairment of decision-making in diseases such as mild cognitive impairment, schizophrenia, anorexia, and obsessive-compulsive disorder is particularly harmful [1–4].

Prior fMRI studies looking at decision-making have suggested involvement of the orbitofrontal cortex (OFC), the dorsolateral prefrontal cortex (dlPFC), and the anterior cingulate cortex (ACC) [5, 6] in making decisions in uncertain conditions. Other implicated regions include the insula, the posterior parietal, the inferior parietal, and inferior temporal areas [6, 7]. Studies have suggested that information about the correct decision is stored in the ventral temporal cortex and posterior parietal cortex [8, 9], whereas the ventromedial pre-frontal cortex (vMPFC) has been implicated in computing expected value and reward outcome in processing decisions [10]. The vMPFC works with the hippocampus during mismatch detection [11]. In addition, the role of the basal ganglia in decision-making, particularly as rules are learned, is becoming increasingly evident. The striatum is involved with reward learning and habitual actions, and activation may correlate with prediction of punishment [10, 12, 13]. A computational model of decision-making as performed by the basal ganglia, developed by Bogacz and Larsen [14], involves a circuit that includes the cortex, striatum, subthalamic nucleus, and globus pallidus. This corresponds to the dorsolateral prefrontal (executive) loop of the basal ganglia [15]. The ACC engages the prefrontal cortex and is implicated in conflict monitoring and outcome evaluation [16]. Clearly, the literature implicates many regions of the brain involved in decision-making under uncertain conditions, and in this study, we will provide a clearer description of the regions of the brain involved, as determined by a simplified paradigm.

The aim of this study was to not only identify brain regions involved in decision-making under conditions of rule uncertainty but also to describe the interactions these brain regions have using network analysis. Our focus was on healthy young individuals in order to gain insights into the complex interactions that are required for successful decision-making in times of rule uncertainty before looking at the impact that age and/or disease can have on this process. We used functional MRI (fMRI) as a non-invasive means for measuring the neuroanatomical activity through the blood oxygenation level-dependent (BOLD) signal

which increases coincident with brain region activation [17]. The BOLD signal is generally accepted as a marker of neural activity, as it changes with blood flow to a given region of the brain and the level of oxygenation of the blood. Other studies that measure responses to uncertainty have used the Iowa Gambling Tasks or tasks that manipulated the levels of uncertainty. The decision-making task that we used allowed for a binary difference to be measured as the rule was either certain (known from first trial) or completely uncertain (changes at every trial). The task conditions were matched such that a comparison of BOLD signal response in the certain and uncertain condition allowed for the comparison of the effect of certainty and uncertainty on various brain regions. We applied a network analysis in order to assess the functional connection between the regions of the brain involved in decision-making.

Methods

Participants

This is a cross-sectional study. Twenty-three healthy participants ages 18–37 were selected (9 males) from the greater Boston community, and the study occurred from August 2015 to March 2016. Participants were recruited for one visit. Eligibility included being under the age of 40 with no neurologic disease or uncorrected vision impairment. Participants signed a consent form approved by the institutional review board. The data from four participants were excluded because of excessive movement artifact, leaving data from 19 participants (7 males) available for analysis.

Paradigm

The task was projected from a personal computer onto a high-resolution screen, which was reflected in a mirror above the participant's face as he or she lay in the MRI. The screen showed a row of five cards on the top and a row at the bottom with a single card (Fig. 1). The participants were instructed to match the bottom card to a card in the top row to the best of their ability, with no further instruction about matching criteria. Responses were recorded using a button box. Each card had five different properties: shape, shape color, background color, number of shapes, and border. Card foreground colors were matched for equal luminance, as were the background colors. Shape sizes and border sizes were equivalent. Each of the top cards matched the bottom card in exactly one attribute. The card-matching screen was presented for 4 s, and participants were instructed to match within those 4 s. Card presentation feedback was shown for 2 s. Feedback was "Correct," "Incorrect," or "Skipped." There were 30 card presentations per run; fixation periods of 30 s were alternated with task periods of 30 s that contained five cycles of card presentation and feedback. The top row remained the same throughout each run, and the bottom card changed. The fixation was a "#" symbol in the middle of the screen, and participants were asked to watch the fixation mark while relaxed, attentive, and awake.

There were two conditions, one in which the rule was certain and one in which the rule was uncertain. In the certain condition, the matching criteria were locked to the first matching rule the participant applied. In the uncertain condition, the matching criteria changed at every single interval. A run of 30 card matches would be entirely either the certain or

uncertain condition, and the six runs alternated between certain and uncertain conditions. The sequence of cards shown was identical for pairs of uncertain and certain conditions. However, the matching rules would be set as described previously. The start condition was varied between participants. Some had the certain condition in runs 1, 3, and 5; some had the certain condition in runs 2, 4, and 6. Subjects were instructed to hold a five-fingered button box in their right hand and to select the button corresponding to their choice. Choices aligned with the finger position (1 left to 5 right).

MRI acquisition and preprocessing

Data were collected using a Phillips 3 T Achieva Scanner and a 32-channel head coil. The scan began with localization and a reference scan, followed by six functional runs of a single-shot echo-planar imaging sequence (TR = 2 s, TE = 35 ms, 30 slices, 3-mm slice thickness, inplane resolution 3 × 3 mm), and finally, T1-weighted (T1W) MP-RAGE sagittal images were acquired (TR/TE = 6.7/3.1 ms; acquisition matrix = 256 × 254, 150 slices; FOV = 250 × 250 × 180 mm; voxel size = 0.98 × 0.98 × 1.2 mm; flip angle = 9°).

Freesurfer software (surfer.nmr.mgh.harvard.edu version 5. 1) was used to parcel and label the structural scans of each of the participants [18]. The software identified gray and white matter regions in the cortex and sub-cortex. Eighty-two gray matter regions were selected from this set for network analysis. The fMRI data were preprocessed with motion correction using MCFLIRT [19], spatial smoothing, and temporal filtering using fMRI Expert Analysis Tool (FEAT; Oxford, UK; v6. 0 http://fsl.fmrib.ox.ac.uk/fsl/fslwiki/FSL). Filtering using FEAT applies a linear high-pass filter to remove low-frequency artifacts [20]. Using FEAT, the fMRI data were registered to both the T1-weighted structural image of the brain, extracted from Freesurfer, and the MNI152 average. The preprocessed fMRI data were labeled using the generated Freesurfer ROIs. A mean time series for each ROI was calculated by averaging all fMRI voxel values within each ROI over time, resulting in 90 time points calculated for each of the 6-min runs. The portions of the time course associated with fixation were removed in order to only correlate task performance.

Networks were constructed with the ROI time series as the nodes and the Pearson correlation coefficients between each pair of nodes as the edges. Network measures were calculated on these constructed networks. Binary measures were calculated on networks constructed by using threshold values ranging from 0.4 to 0.9 of the correlation coefficient. Weighted measures were calculated using the Fisher transformation of the correlation coefficient of the matrix. The measures calculated included network size (the number of suprathreshold edges present in the network), node strength (the sum of the edge weights for each node), and assortativity (the tendency of nodes with similar degree to connect to each other). All of these measures except for size were calculated using the Brain Connectivity Toolbox [21]. In order to assess significance, permutation testing was used. Ten thousand random datasets were constructed by shuffling the edges between participants. Then, the network measures were calculated on each of these generated datasets, and the placement on the distribution of these network measures was assessed in order to calculate the p value.

Data were also analyzed by FEAT (Oxford, UK; v6.0 http://fsl.fmrib.ox.ac.uk/fsl/fslwiki/FSL) which performed statistical analysis using the general linear model (GLM) to calculate

task contribution to the BOLD signal. For each participant and in each run, a GLM was constructed of the blood flow in each voxel in comparing the task condition to the fixation condition. Higher-order FEAT stats were calculated by averaging within each participant for each condition. A paired comparison of a participant's averaged uncertain versus certain condition was calculated using the GLM. *Z*-statistic images were thresholded with clusters in which $Z > 2.3$ and the corrected cluster significance was $p < 0.05$.

Results

FEAT analysis

The GLM analysis determining the contributions of the task to each signal yielded significant differences between the two conditions. In comparing certain > uncertain BOLD signal, the analysis yielded bilateral clusters in the insula that extend into the boundary of the parietal and temporal lobe, as well as a medial frontal cluster (Figs. 2 and 3). The uncertain > certain comparison yielded three large clusters—a midline cluster that extended through the midbrain, the thalamus, bilateral pre-frontal cortex, the striatum, and bilateral clusters that extended through the parietal cortex and occipital cortex (Figs. 4 and 5).

Network analysis

Using a threshold of 0.4–0.9 for binary network measures, we found a number of differences that were consistent across thresholds. Network size was significant at all values with correction for multiple comparisons using the FDR method, except that at threshold 0.8, the network was larger, with a greater number of edges, for the certain condition (Table 1). Network density was significant for all *p* values except 0.7 (Table 1), and assortativity was only significant at threshold 0.7 (Table 1). Node strength had six nodes significantly greater in the certain condition and 20 nodes significantly greater in the uncertain condition (Table 2). The brain networks were visualized with the BrainNet Viewer [22].

Discussion

In this study, we set out to explore how brain activity differs in the process of decision-making when the underlying rule is known (certain) or unknown (uncertain) as a binary outcome. We have found differential brain activity under these two conditions and differences in the network of functional connectivity required to support them. In the uncertain condition, we found a larger, more densely connected network than in the certain condition. Conversely, in the certain condition compared to the uncertain condition, a number of the network nodes showed greater clustering coefficients and node strengths.

Certainty is inherently desirable and uncertainty inherently aversive [23–25]. In our task with only the limited feedback, we saw activation in the reward circuits. During the certain condition, we saw greater activation in the vmPFC and the OFC. The vmPFC has been found to be active in valuating reward [10, 26]. OFC activity has also been found to correlate with reward expectation [27, 28]. We also found increased insula activation, which has been shown to be more active in a decision-making task with a certainty component [29]. We found ROI-based network measures that showed increased connectivity (node strength, as reflected by greater numbers of edges) in the OFC, frontal ROIs, and temporal ROIs.

A meta-analysis conducted by White et al. [6] described that greater activation was observed in the ACC, insula, and dlPFC and posterior parietal cortices in decision-making under uncertain conditions. We found some confirmation of the expected activation of brain regions under uncertain conditions, including activation of the ACC, the dlPFC, and the striatum. Interestingly, the ACC has been implicated in conflict monitoring and anticipation [15, 16]. The ACC is known to engage the dlPFC and contains many reciprocal connections. Likewise, the executive loop of the basal ganglia involves the dlPFC [15]. The striatum is involved with reward-based learning and prediction error, although activation may correlate with punishment [10, 12, 13, 30]. The computational model of decision-making developed by Bogacz and Larsen [14] incorporates the cortex, the striatum, the sub-thalamic nucleus, and the thalamus.

A large parietal and occipital cluster of activation was found in the uncertain condition. Activation of the posterior parietal cortex has been shown to vary as a function of uncertainty [9]. In addition, the lateral intraparietal area has been shown to encode value for saccadic choices in primates [31–33]. This area corresponds to the ventral intraparietal area in humans [15]. Therefore, the activation may correlate with encoding the value of the choice involved.

Unexpectedly, strong midbrain activation was found in the uncertain condition. The midbrain has generally been found to be active in reward [24, 34]; however, there are substantial connections in the direct circuit of the basal ganglia, which involves the substantia nigra and the striatum [15]. The direct circuit is a motor circuit, and it could be that greater motor control is required in this task because of the increased uncertainty. In addition, the increased activation of the occipital cortex in the uncertain condition was unexpected, given the equally visual nature of the certain and uncertain conditions.

ROIs reflecting greater network connectivity in the uncertain condition include the amygdala and hippocampus, as well as the frontal and parietal regions that were discussed previously. The amygdala is thought to encode emotional valence [35, 36], and because uncertainty correlates to increased anxiety and worry [37, 38], this may correspond to the negative emotions that occur during uncertainty. The hippocampus is generally active during memory tasks and is also thought to help in valuating outcomes [39]. While this suggests a reward encoding, there are also substantial connections between the hippocampus and the amygdala [15], so it logically follows that if one is highly functionally connected to other brain regions, the other will also be highly connected. In addition, because of the memory capabilities required to discard and update the rule choices in the uncertain condition, the coincident activation of the hippocampus is expected. Using network analysis allows us to reduce the amount of inter-subject variability, because each ROI is determined based on each participant’s neuroanatomy—hereby limiting the influence in population analysis of larger or smaller brain regions contributing to activity. As such, the network measures determined in this study provide baseline markers on which uncertain decision-making in pathologic populations might be compared.

Taken together, these results reinforce many studies of decision-making under conditions of rule uncertainty versus rule certainty as well as include new information about differences in

the brain's behavior between these two conditions. The involvement of the insula, parietal cortex, temporal cortex, ventromedial prefrontal cortex, and orbitofrontal cortex of the certain condition is generally associated with rule certainty, reward, and behavioral flexibility [6, 9, 40]. The activation of areas related to reward reinforces the notion that certainty is inherently rewarding. The widespread activation in the uncertain condition included the prefrontal cortex, the striatum, the thalamus, the midbrain, the amygdala, the hippocampus, and the parietal cortex and occipital cortex. While the prefrontal cortex, parietal cortex, striatum, thalamus, amygdala, and hippocampal involvement were expected, the occipital cortical involvement and the midbrain involvement were less expected. The increased involvement of these regions may be attributed to increased visual attention and increased motor control perhaps through a "top-down" process attempted to remove uncertainty through increased vigilance.

Effective decision-making is a vital process for independent living. It requires the integration of information provided by the senses to that found in the knowledge stores in the brain in order to extract a rule that will bring about the desired outcome. In this study, we have furthered our understanding of this process by affirming regional brain activity during a decision-making task and then expanding our understanding of this process by looking at the network of activity that supports this function. We are comforted to see systems such as the reward system being more actively involved during the certain conditions and a bit perplexed by some of the regions and network findings under uncertain conditions. We validated a novel decision-making task as an appropriate means to measure uncertainty, and in the future, we can expand on this by including disease populations. Limitations include the fact that we did not pre or post interview the population and thus did not collect educational data or discuss task strategy for participants this task. Although more work remains for us to clearly understand how the brain accomplishes this vital task, this initial study provides clarity to the current body of literature.

Acknowledgments

Funding This study was funded by departmental funds from the Department of Anatomy and Neurobiology at the Boston University School of Medicine.

References

1. Triebel K, Martin R, Griffith H, Marceaux J, Okonkwo O, Harrell L, Clark D, Brockington J, Bartolucci A, Marson DC. Declining financial capacity in mild cognitive impairment. Neurology. 2009; 73(12):928–934. https://doi.org/10.1212/WNL.0b013e3181b87971. [PubMed: 19770468]
2. Matsuzawa D, Shirayama Y, Niitsu T, Hashimoto K, Iyo M. Deficits in emotion based decision-making in schizophrenia; a new insight based on the Iowa Gambling Task. Prog Neuro-Psychopharmacol Biol Psychiatry. 2015; 57:52–59. https://doi.org/10.1016/j.pnpbp.2014.10.007.
3. Zhang L, Dong Y, Ji Y, Zhu C, Yu F, Ma H, Chen X, Wang K. Dissociation of decision making under ambiguity and decision making under risk: a neurocognitive endophenotype candidate for obsessive-compulsive disorder. Prog Neuro-Psychopharmacol Biol Psychiatry. 2015; 57:60–68. https://doi.org/10.1016/j.pnpbp.2014.09.005.
4. Ritschel F, Geisler D, King JA, Bernardoni F, Seidel M, Boehm I, Vettermann R, Biemann R, Roessner V, Smolka MN, Ehrlich S. Neural correlates of altered feedback learning in women recovered from anorexia nervosa. Sci Rep. 2017; 7(1):5421. https://doi.org/10.1038/s41598-017-04761-y. [PubMed: 28710363]

5. Demanuele C, Kirsch P, Esslinger C, Zink M, Meyer-Lindenberg A, Durstewitz D. Area-specific information processing in prefrontal cortex during a probabilistic inference task: a multivariate fMRI BOLD time series analysis. PLoS One. 2015; 10(8):e0135424. https://doi.org/10.1371/journal.pone.0135424. [PubMed: 26258487]
6. White TP, Engen NH, Sørensen S, Overgaard M, Shergill SS. Uncertainty and confidence from the triple-network perspective: voxel-based meta-analyses. Brain Cogn. 2014; 85:191–200. https://doi.org/10.1016/j.bandc.2013.12.002. [PubMed: 24424423]
7. Krug A, Cabanis M, Pyka M, Pauly K, Walter H, Landsberg M, Shah NJ, Winterer G, Wölwer W, Musso F, Müller BW, Wiedemann G, Herrlich J, Schnell K, Vogeley K, Schilbach L, Langohr K, Rapp A, Klingberg S, Kircher T. Investigation of decision-making under uncertainty in healthy subjects: a multi-centric fMRI study. Behav Brain Res. 2014; 261:89–96. https://doi.org/10.1016/j.bbr.2013.12.013. [PubMed: 24355752]
8. Philiastides MG, Biele G, Heekeren HR. A mechanistic account of value computation in the human brain. Proc Natl Acad Sci. 2010; 107(20):9430–9435. https://doi.org/10.1073/pnas.1001732107. [PubMed: 20439711]
9. Hutchinson JB, Uncapher MR, Wagner AD. Increased functional connectivity between dorsal posterior parietal and ventral occipitotemporal cortex during uncertain memory decisions. Neurobiol Learn Mem. 2015; 117:71–83. https://doi.org/10.1016/j.nlm.2014.04.015. [PubMed: 24825621]
10. Daw ND, Doya K. The computational neurobiology of learning and reward. Curr Opin Neurobiol. 2006; 16(2):199–204. https://doi.org/10.1016/j.conb.2006.03.006. [PubMed: 16563737]
11. Garrido MI, Barnes GR, Kumaran D, Maguire EA, Dolan RJ. Ventromedial prefrontal cortex drives hippocampal theta oscillations induced by mismatch computations. NeuroImage. 2015; 120:362–370. https://doi.org/10.1016/j.neuroimage.2015.07.016. [PubMed: 26187453]
12. Stalnaker TA, Calhoon GG, Ogawa M, Roesch MR, Schoenbaum G. Reward prediction error signaling in posterior dorsomedial striatum is action specific. J Neurosci. 2012; 32(30):10296–10305. https://doi.org/10.1523/JNEUROSCI.0832-12.2012. [PubMed: 22836263]
13. Samejima K, Ueda Y, Doya K, Kimura M. Representation of action-specific reward values in the striatum. Science. 2005; 310(5752):1337–1340. https://doi.org/10.1126/science.1115270. [PubMed: 16311337]
14. Bogacz R, Larsen T. Integration of reinforcement learning and optimal decision-making theories of the basal ganglia. Neural Comput. 2011; 23(4):817–851. https://doi.org/10.1162/NECO_a_00103. [PubMed: 21222528]
15. Nieuwenhuys, R., Voogd, J., van Huijzen, FMAAC. The human central nervous system. Springer; Berlin Heidelberg: 2008.
16. Botvinick MM. Conflict monitoring and decision making: reconciling two perspectives on anterior cingulate function. Cogn Affect Behav Neurosci. 2007; 7(4):356–366. https://doi.org/10.3758/CABN.7.4.356. [PubMed: 18189009]
17. Logothetis NK. The neural basis of the blood-oxygen-level-dependent functional magnetic resonance imaging signal. Philos Trans R Soc Lond Ser B Biol Sci. 2002; 357(1424):1003–1037. https://doi.org/10.1098/rstb.2002.1114. [PubMed: 12217171]
18. Desikan RS, Ségonne F, Fischl B, Quinn BT, Dickerson BC, Blacker D, Buckner RL, Dale AM, Maguire RP, Hyman BT, Albert MS, Killiany RJ. An automated labeling system for subdividing the human cerebral cortex on MRI scans into gyral based regions of interest. NeuroImage. 2006; 31(3):968–980. https://doi.org/10.1016/j.neuroimage.2006.01.021. [PubMed: 16530430]
19. Jenkinson M, Bannister P, Brady M, Smith S. Improved optimization for the robust and accurate linear registration and motion correction of brain images. NeuroImage. 2002; 17(2):825–841. https://doi.org/10.1006/nimg.2002.1132. [PubMed: 12377157]
20. Smith SM, Jenkinson M, Woolrich MW, Beckmann CF, Behrens TEJ, Johansen-Berg H, Bannister PR, de Luca M, Drobnjak I, Flitney DE, Niazy RK, Saunders J, Vickers J, Zhang Y, de Stefano N, Brady JM, Matthews PM. Advances in functional and structural MR image analysis and implementation as FSL. NeuroImage. 2004; 23(Suppl 1):S208–S219. https://doi.org/10.1016/j.neuroimage.2004.07.051. [PubMed: 15501092]

21. Rubinov M, Sporns O. Complex network measures of brain connectivity: uses and interpretations. NeuroImage. 2010; 52(3):1059–1069. https://doi.org/10.1016/j.neuroimage.2009.10.003. [PubMed: 19819337]
22. Xia M, Wang J, He Y. BrainNet Viewer: a network visualization tool for human brain connectomics. PLoS One. 2013; 8(7):e68910. https://doi.org/10.1371/journal.pone.0068910. [PubMed: 23861951]
23. Bach, DR., Pryce, CR., Seifritz, E. The experimental manipulation of uncertainty. In: Raber, J., editor. Animal models of behavioral analysis. Humana Press; Totowa: 2011. p. 193-216.https://doi.org/10.1007/978-1-60761-883-6_8
24. Reuman L, Jacoby RJ, Fabricant LE, Herring B, Abramowitz JS. Uncertainty as an anxiety cue at high and low levels of threat. J Behav Ther Exp Psychiatry. 2015; 47:111–119. https://doi.org/10.1016/j.jbtep.2014.12.002. [PubMed: 25562749]
25. Zhang H, Daw ND, Maloney LT. Human representation of visuo-motor uncertainty as mixtures of orthogonal basis distributions. Nat Neurosci. 2015; 18(8):1152–1158. https://doi.org/10.1038/nn.4055. [PubMed: 26120962]
26. Bengtsson SL, Haynes J-D, Sakai K, Buckley MJ, Passingham RE. The representation of abstract task rules in the human pre-frontal cortex. Cereb Cortex. 2009; 19(8):1929–1936. https://doi.org/10.1093/cercor/bhn222. [PubMed: 19047573]
27. Kepecs A, Uchida N, Zariwala HA, Mainen ZF. Neural correlates, computation and behavioural impact of decision confidence. Nature. 2008; 455(7210):227–231. https://doi.org/10.1038/nature07200. [PubMed: 18690210]
28. Klein-Flügge MC, Barron HC, Brodersen KH, et al. Segregated encoding of reward-identity and stimulus-reward associations in human orbitofrontal cortex. J Neurosci. 2013; 33(7):3202–3211. https://doi.org/10.1523/JNEUROSCI.2532-12.2013. [PubMed: 23407973]
29. Bhanji JP, Beer JS, Bunge SA. Taking a gamble or playing by the rules: dissociable prefrontal systems implicated in probabilistic versus deterministic rule-based decisions. NeuroImage. 2010; 49(2):1810–1819. https://doi.org/10.1016/j.neuroimage.2009.09.030. [PubMed: 19781652]
30. Klein TA, Ullsperger M, Jocham G. Learning relative values in the striatum induces violations of normative decision making. Nat Commun. 2017; 8:16033. https://doi.org/10.1038/ncomms16033. [PubMed: 28631734]
31. Kiani R, Shadlen MN. Representation of confidence associated with a decision by neurons in the parietal cortex. Science. 2009; 324(5928):759–764. https://doi.org/10.1126/science.1169405. [PubMed: 19423820]
32. Beck JM, Ma WJ, Kiani R, Hanks T, Churchland AK, Roitman J, Shadlen MN, Latham PE, Pouget A. Probabilistic population codes for Bayesian decision making. Neuron. 2008; 60(6):1142–1152. https://doi.org/10.1016/j.neuron.2008.09.021. [PubMed: 19109917]
33. Andersen RA, Cui H. Intention, action planning, and decision making in parietal-frontal circuits. Neuron. 2009; 63(5):568–583. https://doi.org/10.1016/j.neuron.2009.08.028. [PubMed: 19755101]
34. Zhang W, Schneider DM, Belova MA, Morrison SE, Paton JJ, Salzman CD. Functional circuits and anatomical distribution of response properties in the primate amygdala. J Neurosci. 2013; 33(2):722–733. https://doi.org/10.1523/JNEUROSCI.2970-12.2013. [PubMed: 23303950]
35. Berntson GG, Bechara A, Damasio H, Tranel D, Cacioppo JT. Amygdala contribution to selective dimensions of emotion. Soc Cogn Affect Neurosci. 2007; 2(2):123–129. https://doi.org/10.1093/scan/nsm008. [PubMed: 18414599]
36. Styliadis C, Ioannides AA, Bamidis PD, Papadelis C. Amygdala responses to valence and its interaction by arousal revealed by MEG. Int J Psychophysiol. 2014; 93(1):121–133. https://doi.org/10.1016/j.ijpsycho.2013.05.006. [PubMed: 23688672]
37. de Bruin G, Rassin E, Muris P. Worrying in the lab: does intolerance of uncertainty have predictive value? Behav Chang. 2006; 23(02):138–147. https://doi.org/10.1375/bech.23.2.138.
38. Rosen NO, Knäuper B. A little uncertainty goes a long way: state and trait differences in uncertainty interact to increase information seeking but also increase worry. Health Commun. 2009; 24(3):228–238. https://doi.org/10.1080/10410230902804125. [PubMed: 19415555]

39. Lebreton M, Bertoux M, Boutet C, Lehericy S, Dubois B, Fossati P, Pessiglione M. A critical role for the hippocampus in the valuation of imagined outcomes. PLoS Biol. 2013; 11(10):e1001684. https://doi.org/10.1371/journal.pbio.1001684. [PubMed: 24167442]

40. Tei S, Fujino J, Kawada R, Jankowski KF, Kauppi JP, van den Bos W, Abe N, Sugihara G, Miyata J, Murai T, Takahashi H. Collaborative roles of temporoparietal junction and dorsolateral prefrontal cortex in different types of behavioural flexibility. Sci Rep. 2017; 7(1):6415. https://doi.org/10.1038/s41598-017-06662-6. [PubMed: 28743978]

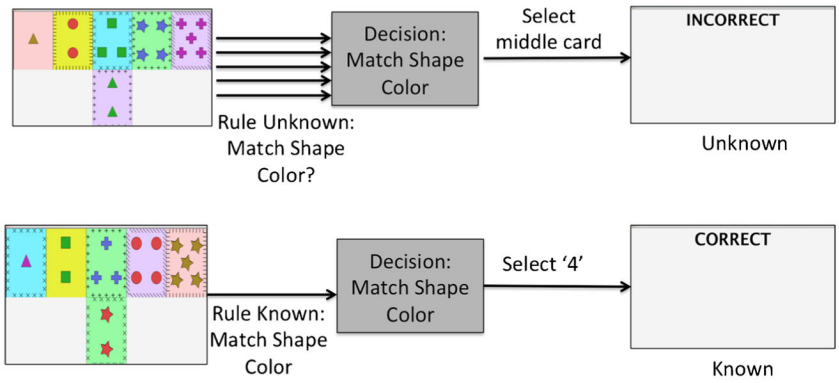

Fig. 1.

Decision-making paradigm. The screen showed five cards to choose from at the top, with a card to match at the bottom. Participants were not given any information about which rule to apply. In the rule-uncertain condition, the rule changed at every interval. In the rule-certain condition, the rule was locked to the participant's first choice and stayed the same for the entire duration

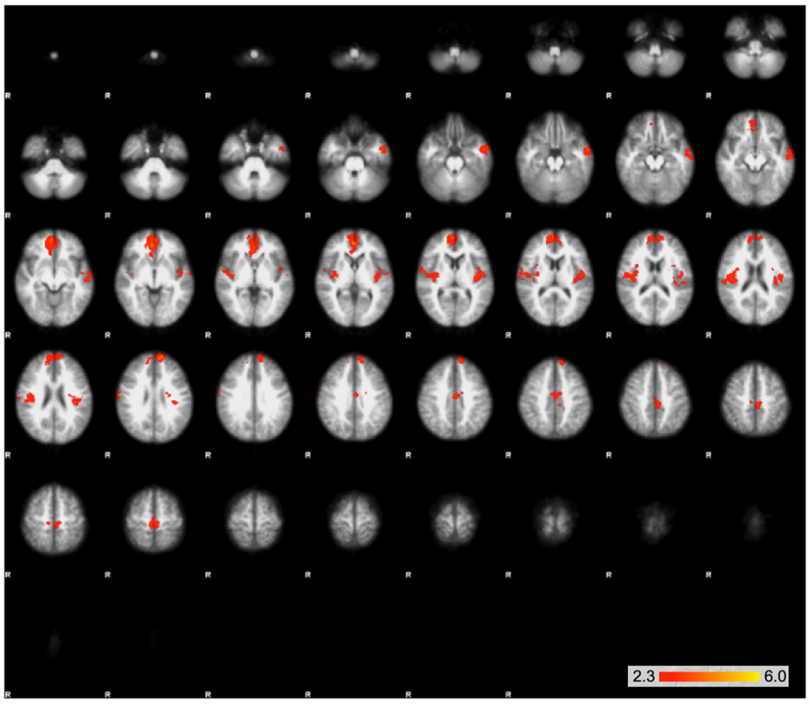

Fig. 2.

Large clusters of activation that were significantly greater in the certain than the uncertain condition as determined by the GLM using FEAT. Clusters are shown on serial axial slices, with z score reflected by color bar. There were three significantly different clusters extending bilaterally from the insula into the parietal/temporal boundary, as well as a single midline frontal cluster

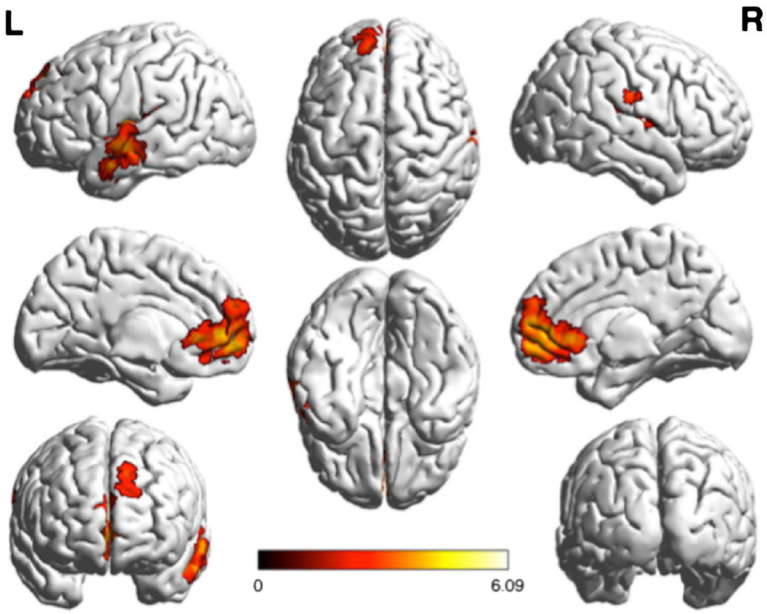

Fig. 3.

Regions demonstrating greater activation in the certain condition than in the uncertain condition, projected onto a surface model of the brain [22]

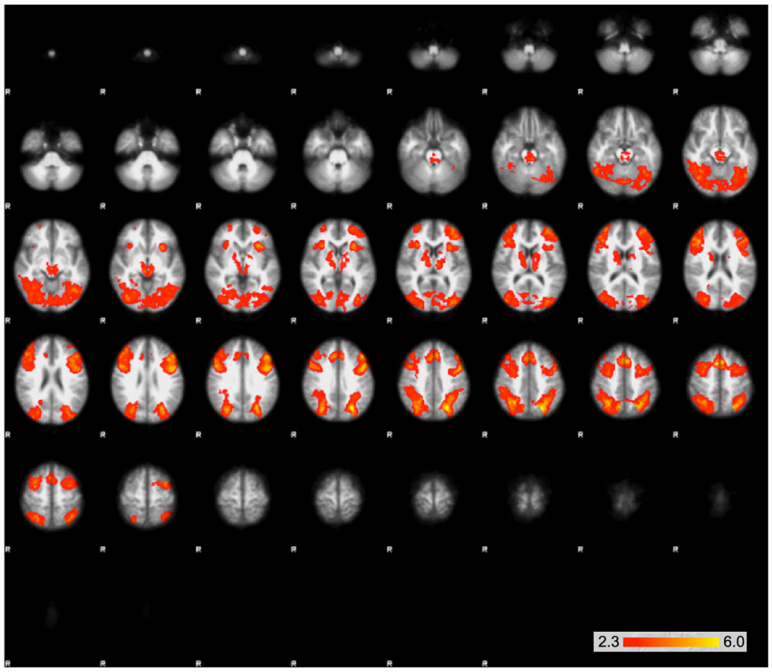

Fig. 4.

Large clusters of activation that were significantly greater in the uncertain than the certain condition as determined by the GLM using FEAT. Clusters are shown on serial axial slices, with z score reflected by color bar. There were three significant clusters, extending through the midbrain, thalamus, bilateral prefrontal cortex, striatum, as well as bilateral clusters extending through the parietal and occipital cortex

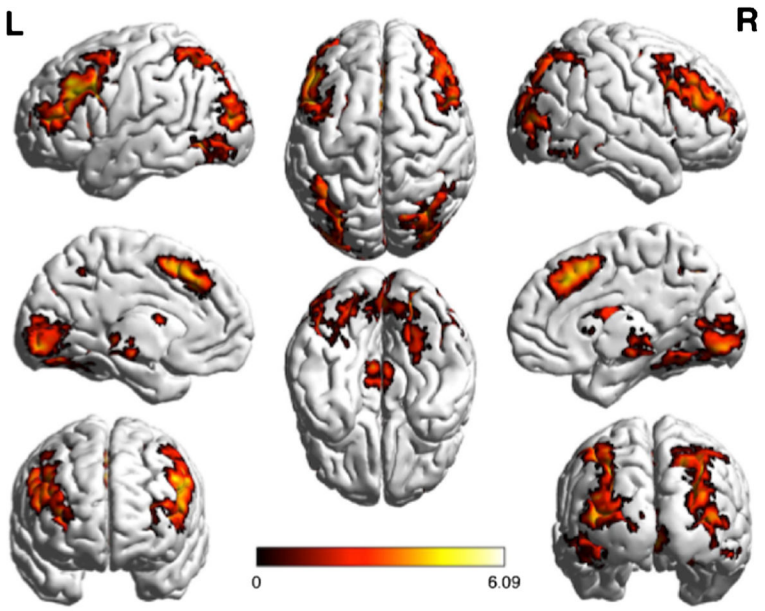

Fig. 5.

Regions demonstrating greater activation in the uncertain condition than in the certain condition, projected onto a surface model of the brain [22]

Table 1

Comparisons of network measures for the uncertain and certain conditions, using different threshold values of the Pearson correlation coefficient in order to calculate the network value

Threshold	Certain mean	Uncertain mean	*p* value
Network size			
0.4	3335	*3915*	< 0.0001
0.5	2279	*2363*	< 0.0001
0.6	1367	*1429*	< 0.0001
0.7	692	*704*	0.0052
0.8	281	269	0.0001
Network density			
0.4	0.56	*0.57*	0.0002
0.5	0.38	*0.4*	< 0.0001
0.6	0.23	*0.24*	< 0.0001
0.7	0.12	0.12	0.24
0.8	*0.056*	0.054	< 0.0001
Network assortativity			
0.4	0.0817	0.0728	0.14
0.5	0.15	0.15	0.27
0.6	0.23	0.22	0.18
0.7	*0.28*	*0.32*	*0.0031*
0.8	0.08	0.07	0.14

Italicized numbers reflect those that are significantly greater

Table 2

Node strength (sum of weighted edges) showing significant difference between certain and uncertain conditions. *p* values were determined to be significant after adjusting for multiple comparisons (number of nodes)

ROI	Certain mean	Uncertain mean	*p* value
a. ROIs for which the strength is greater for the certain than the uncertain condition			
Right pallidum	33.90	32.27	0.001
Left frontal ole	21.89	18.78	< 0.0001
Left lateral occipital	40.74	39.06	0.0016
Left medial orbital frontal	32.06	30.37	0.0015
Left rostral anterior cingulate	37.54	35.49	0.0003
Left transverse temporal	38.23	36.63	0.0013
Right frontal pole	25.37	22.40	< 0.0001
Right lateral occipital	40.48	38.71	0.0011
Right lateral orbitofrontal	33.61	31.87	0.0003
Right temporal pole	23.10	19.75	< 0.0001
b. ROIs for which the strength is greater for the uncertain than the certain condition			
Left amygdala	29.13	31.63	< 0.0001
Left pallidum	30.24	31.65	0.0044
Right accumbens	22.76	24.23	0.0028
Right amygdala	20.82	22.77	< 0.0001
Right hippocampus	33.89	35.54	0.0015
Left cuneus	43.48	45.94	0.0002
Left inferior parietal	44.69	47.38	< 0.0001
Left insula	42.78	44.36	0.0032
Left parahippocampal	22.15	24.91	< 0.0001
Left precuneus	47.76	50.39	< 0.0001
Left superior frontal	52.10	54.23	0.0004
Left temporal pole	23.65	25.02	0.0018
Right caudal anterior cingulate	44.54	46.45	0.001
Right isthmus cingulate	42.73	44.38	0.0021
Right parahippocampal	30.92	32.48	0.0008
Right precuneus	49.37	51.22	0.0016